Dyes and Pigments 92 (2012) 1223–1230

Contents lists available at ScienceDirect

Dyes and Pigments

journal homepage: www.elsevier.com/locate/dyepig

Synthesis, characterization, and optical properties of new metal complexes with the multi-sulfur 1,2-dithiolene ligand

Liang Hu [a], Jie Qin [a], Nan Zhou [a], Yi-Fei Meng [a], Yan Xu [b], Jing-Lin Zuo [a,*], Xiao-Zeng You [a]

[a] State Key Laboratory of Coordination Chemistry, School of Chemistry and Chemical Engineering, Nanjing National Laboratory of Microstructures, Nanjing University, Nanjing 210093, PR China
[b] State Key Laboratory of Materials-Oriented Chemical Engineering, College of Chemistry and Chemical Engineering, Nanjing University of Technology, Nanjing 210009, PR China

ARTICLE INFO

Article history:
Received 5 May 2011
Received in revised form
30 July 2011
Accepted 1 August 2011
Available online 17 August 2011

Keywords:
Synthesis
Metal complexes
Near-IR dyes
Multi-sulfur ligand
Crystal structures
Optical properties

ABSTRACT

Metal complexes containing a new multi-sulfur atom containing 1,2-dithiolene ligand, [4′,5′:5,6] [1,4] dithiino[2,3-*b*] quinoxaline-1′,3′-dithiolate, have been synthesized and characterized by electrochemical measurements, IR, UV–NIR and ESR spectroscopies. X-ray structure analysis reveals that the anions of the Ni-complex derived from the new ligand form a zig-zag chain along the *b* axis, and the anions of Au complex of the ligand stack along the *a* axis while the cations occupy the holes. The Ni-complex exhibits remarkable absorption at 1082 nm ($\varepsilon = 15\,000$ dm^3 mol^{-1} cm^{-1}) and good solubility that render this complex as a promising near-IR dye for Q-switching neodymium lasers. The third-order non-linear optical properties of the complexes are measured by the *Z*-scan technique with a 6.5 ns pulsed laser at 532 nm. The Au complexes exhibit non-linear optical absorptive abilities, while the non-linear absorption of the nickel complex is negligible. All of the complexes show effective self-defocusing performance. The third-order non-linear optical susceptibilities for the Au complexes have been determined to be of the order of 10^{-13} esu.

1. Introduction

Metal complexes of bis(dithiolene) have been extensively studied for their interesting properties and applications in areas such as conductivity, magnetism, near-infrared dyes, and non-linear optical materials [1–13]. They exhibit strong absorption bands in the near-infrared region in their electronic spectra. They are also known to be very stable to intense irradiation in the IR region and for example are particularly suited for Q-switching lasers (such as Nd–YAG lasers, operating at 1064 nm) [14,15]. This is important in creating materials with intense absorptions in the 1060–1600 nm region to be employed in the application of NIR dyes in Q-switching infrared lasers [8]. In order to be exploited as saturable absorbers, dyes have to satisfy several criteria [16]. In particular, (i) the fundamental absorption should exhibit a very high cross-section at the laser emission wavelength, (ii) no excited-state absorption should be presented at the same wavelength, and (iii) the molecules should be very stable when exposed to light. Moreover, in order to prevent damage to laser optics, the dyes must be quite soluble in inert solvents.

In this paper, four new metal complexes based on the multi-sulfur dithiolene ligand L (L = [4′,5′:5,6] [1,4] dithiino[2,3-*b*] quinoxaline-1′,3′-dithiolate), $[n\text{-Bu}_4\text{N}]_n[\text{Ni(L)}_2]$ ($n = 1$, **1**; $n = 0$, **2**) and $[\text{R}_4\text{N}][\text{Au(L)}_2]$ (R = *n*-Bu, **3**; R = Et, **4**), are synthesized and characterized. Their third-order non-linear optical properties have been studied by using the *Z*-scan method. Importantly, the nickel complex **1** exhibits a strong absorption in the near-infrared region ($\lambda = 1082$ nm, $\varepsilon = 15\,000$ dm^3 mol^{-1} cm^{-1}), which is close to 1064 nm and 1079 nm at which Q-switching Nd–YAG and Nd–YAP lasers operate, respectively.

2. Experimental

2.1. Materials and physical measurements

4,5-Bis(benzoylthio)-1,3-dithiole-2-thione (**I**) was synthesized according to the literature method [17]. All solvents were dried by standard techniques prior to use.

Elemental analyses for C, H and N were determined using a Perkin–Elmer 240C analyzer. Infrared spectra were recorded in the 400–4000 cm^{-1} region by Vector22 Bruker spectrophotometer with KBr pellets. UV–vis spectra were obtained on a UV–3100 spectrophotometer. ESR spectra were recorded on a Bruker ER 200-D-SRC spectrometer. Cyclic voltammetry was performed using

* Corresponding author. Fax: +86 25 83314502.
E-mail address: zuojl@nju.edu.cn (J.-L. Zuo).

0143-7208/$ – see front matter © 2011 Elsevier Ltd. All rights reserved.
doi:10.1016/j.dyepig.2011.08.003

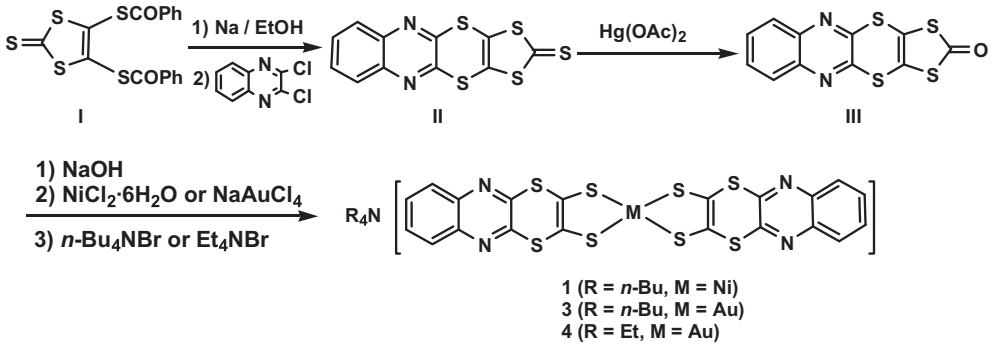

Scheme 1. The synthetic route of complexes **1**, **3** and **4**.

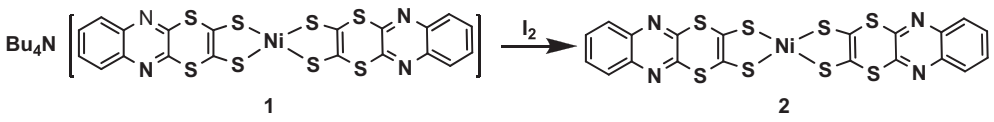

Scheme 2. The synthetic route of complex **2**.

a model 79-1 V-A analyzer with an electrochemical cell using a platinum wire as the working electrode, a platinum plate as the auxiliary electrode and an SCE as the reference electrode.

2.2. Syntheses

2.2.1. Preparation of compound *II*

This compound was prepared by the modified literature method [18]. Under a nitrogen atmosphere, to the suspension of **I** (16.2 g, 40 mmol) in ethanol (20 mL) was added a solution of Na (1.86 g) in ethanol (10 mL). The mixture turned red immediately. 0.5 h later, tetrahydrofuran (50 mL) was added, and then 2,3-dichloroquinoxaline (7.96 g, 40 mmol) was added in one portion. The reaction mixture was stirred at room temperature overnight. The yellow precipitate formed was collected by filtration. The products were washed with water and methanol, and yellow crystals were obtained after recrystallization from toluene. Yield: 78%. Anal. Calcd for $C_{11}H_4N_2S_5$: C, 40.72; H, 1.24; N, 8.63. Found: C, 40.68; H, 1.26; N, 8.65%. IR (KBr, cm^{-1}): 1076 (C═S). EI-MS, *m*/*z*: 323.8 (M^+).

2.2.2. Preparation of compound III

To the thione **II** (810 mg, 2.5 mmol) in chloroform (210 mL) was added mercury(II) acetate (2.8 g) in glacial acetic acid (70 mL). The mixture was stirred at room temperature for 6 h. After filtration, the filtrate was washed with saturated $NaHCO_3$ and then with water. The organic phase was dried with sodium sulfate and concentrated by rotary evaporation. Pale yellow crystals of **III** were obtained by recrystallization from ethanol–chloroform (3:1). Yield: 70%. Anal. Calcd for $C_{11}H_4N_2OS_4$: C, 42.84; H, 1.31; N, 9.08; O, 5.19. Found: C, 42.78; H, 1.29; N, 9.10; O, 5.12%. IR (KBr, cm^{-1}): 1688 (C═O). EI-MS: *m*/*z* 307.8 (M^+).

2.2.3. Preparation of (n-Bu_4N)[$Ni(L)_2$] (*1*)

Under a N_2 atmosphere, an ethanol solution of NaOH (44 mg, 1.1 mmol) was added to a slurry of compound **III** (154 mg, 0.5 mmol) in ethanol (5 mL). To the clear orange solution,

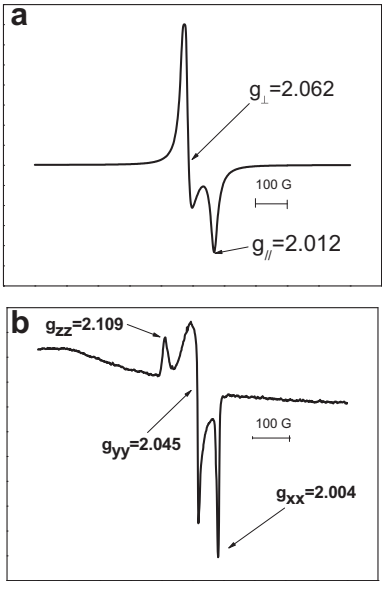

Fig. 1. (a) Powder ESR spectrum and (b) DMF frozen glass ESR spectrum of complex **1** at 110 K.

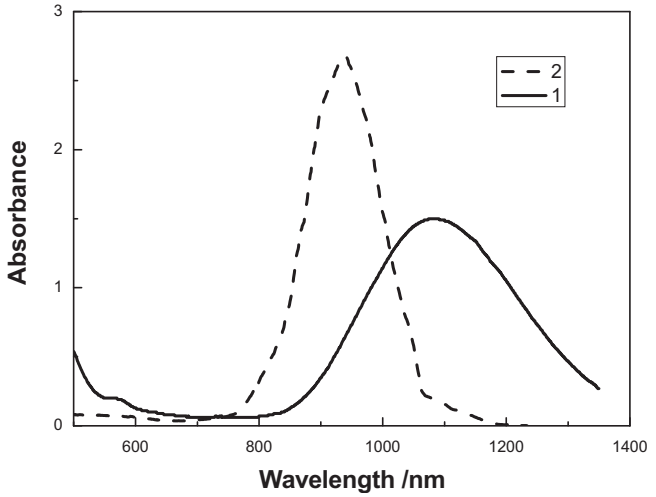

Fig. 2. Absorption spectra of **1** (1×10^{-4} M) in dimethylformamide and **2** (5.2×10^{-5} M) in benzene solution.

Table 1
Absorbance and absorption maxima of some nickel bis(dithiolene) complexes.

Complexes	Solvents	λ_{max}/nm	ε/dm^3 mol^{-1} cm^{-1}	Ref.
[*n*-Bu$_4$N][Ni(L)$_2$]	DMF	1082	15 000	This work
[Ni(L)$_2$]	Benzene	939	53 500	This work
[*n*-Bu$_4$N][Ni(phdt)$_2$]	CH_3CN	1172	15 000	9
[Ni(phdt)$_2$]	Benzene	1028	43 000	9
[*n*-Bu$_4$N][Ni(bddt)$_2$]	CH_3CN	1180	16 800	10
[Ni(phdt)$_2$]	Benzene	1035	63 000	10
[*n*-Bu$_4$N][Ni(dmit)$_2$]	CH_3CN	1137	45 000	9
[*n*-Bu$_4$N][Ni(dddt)$_2$]	CH_3CN	1175	15 600	9
[*n*-Bu$_4$N][Ni(L^{Bu})(L^{Bu})]	CH_2Cl_2	890	15 000	13

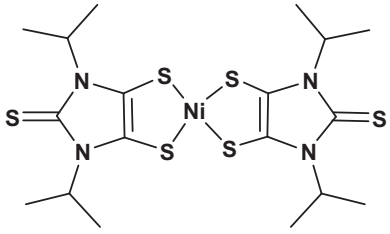

Scheme 3. The structure of [Ni(Pr$^i_2$timdt)$_2$].

$NiCl_2 \cdot 6H_2O$ (59 mg, 0.25 mmol) in ethanol (5 mL) was added dropwise. After 2 h, the solution was stirred in air for additional 30 min. The solution changed from purple to brown as the reaction proceeded. After filtration, *n*-Bu$_4$NBr (0.75 mmol, 250 mg) in ethanol (4 mL) was added to the filtrate. Brown solids were collected by filtration and recrystallized from acetone. Yield: 55%. Calcd for $C_{36}H_{44}N_5NiS_8$: C, 50.16; H, 5.14; N, 8.12. Found: C, 50.09; H, 5.18; N, 8.19%. IR (KBr, cm^{-1}): 2956w, 2869w, 1555m, 1474m, 1328s, 1174s, 1110s, 871m, 755m, 597m, 467m.

2.2.4. Preparation of [Ni(L)$_2$] (**2**)

An acetonitrile solution of I_2 (28 mg, 0.11 mmol) was added to complex **1** (86 mg, 0.1 mmol) in acetonitrile (10 mL). The black powder formed was collected by filtration and washed with acetonitrile. Yield: 70%. Calcd for $C_{20}H_8N_4NiS_8$: C, 38.77; H, 1.30; N, 9.04. Found: C, 38.69; H, 1.37; N, 9.09%. IR (KBr, cm^{-1}): 2920w, 1304s, 1259s, 1176s, 1115s, 754m, 669m, 478m, 420m.

2.2.5. Preparation of (*n*-Bu$_4$N)[Au(L)$_2$] (**3**)

A similar procedure as that used for the preparation of **1** was adopted using sodium tetrachloroaurate(III) (99.5 mg, 0.25 mmol) instead of $NiCl_2 \cdot 6H_2O$. An orange solid was obtained. Yield: 41%. Calcd for $C_{36}H_{44}N_5AuS_8$: C, 43.23; H, 4.43; N, 7.00. Found: C, 43.15; H, 4.41; N, 7.09%. IR (KBr, cm^{-1}): 2958w, 2870w, 1477s, 1379s, 1333m, 1176s, 1111s, 870m, 760m, 597m, 473m.

2.2.6. Preparation of (Et$_4$N)[Au(L)$_2$] (**4**)

A similar procedure as that used for the preparation of **3** was adopted using Et$_4$NBr (0.75 mmol, 158 mg) instead of *n*-Bu$_4$NBr. An orange solid was obtained. Yield: 31%. Calcd for $C_{28}H_{28}N_5AuS_8$: C, 37.87; H, 3.18; N, 7.89. Found: C, 37.79; H, 3.17; N, 7.97%. IR (KBr, cm^{-1}): 2999w, 2977m, 1559m, 1459s, 1410s, 1315m, 1181s, 1113s, 870m, 759m, 598m, 472m.

2.3. Structure determination

The X-ray diffraction data were collected on a Bruker Smart Apex CCD diffractometer equipped with graphite monochromated Mo Kα ($\lambda = 0.71073$ Å) radiation using a ω–2θ scan mode at 291 K. The highly redundant data sets were reduced using *SAINT* [19] and corrected for Lorentz and polarization effects. Absorption corrections were applied using *SADABS* [20] supplied by Bruker. The structure was solved by direct methods and refined by full-matrix least-squares methods on F^2 using *SHELXTL-97* [21]. All non-hydrogen atoms were found in alternating difference Fourier syntheses and least-squares refinement cycles and, during the final cycles, refined anisotropically. Hydrogen atoms were placed in calculated positions and refined as riding atoms with a uniform value of U_{iso}.

The supplementary crystallographic data for this paper are provided in CCDC 806193 (complex **1**) and CCDC 806194 (complex **3**) and can be obtained free of charge via http://www.ccdc.cam.ac.uk/conts/retrieving.html, or from the Cambridge Crystallographic Data Centre, 12 Union Road, Cambridge CB2 1EZ, UK; fax: (+44) 1223-336-033; e-mail: deposit@ ccdc.cam.ac.uk.

2.4. Non-linear optical (NLO) measurements

A dimethylformamide (DMF) solution of each metal complex with a concentration of 2×10^{-4} M contained in a 2 mm thick

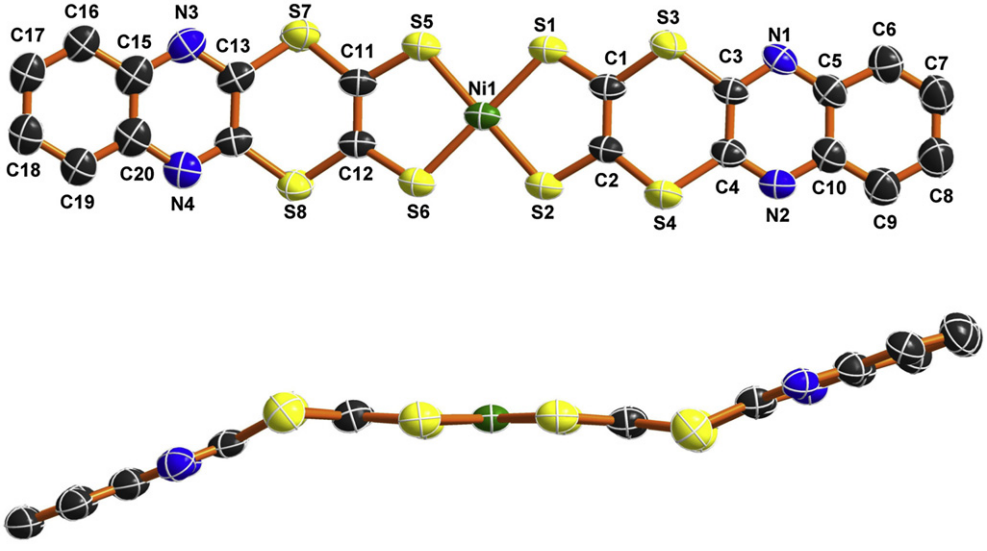

Fig. 3. Top and side views of [Ni(L)$_2$]$^-$ with thermal ellipsoids at 30% probability level. Hydrogen atoms are omitted for clarity.

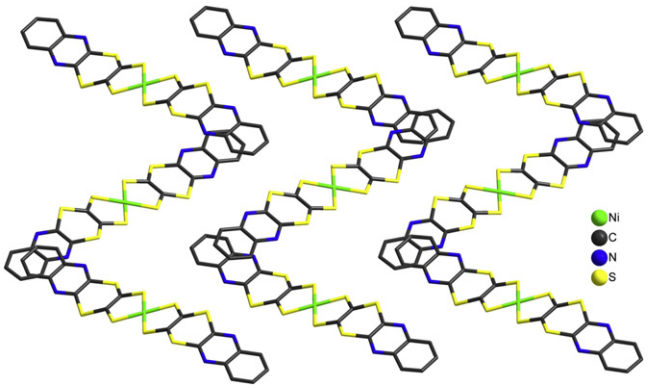

Fig. 4. The packing diagram of the anions of complex **1** looking along the *a* axis.

quartz cuvette was irradiated by a Q-switched frequency-doubled Nd:YAG laser, which produced linearly polarized 6.5 ns (full width at half maximum, FWHM) optical pulses at 532 nm. The laser was operated at a pulse repetition rate of 10 Hz. The laser beam was focused with a 30 cm focal length focusing mirror. The incident and transmitted pulse energies were measured simultaneously by two energy detectors (Rjp-735 energy probes, Laser Precision). The NLO properties of the samples were manifested by moving the samples along the axis of the incident laser irradiance beam (*Z* direction) with respect to the focal point and with incident laser irradiance kept constant (*Z*-scan methods). The transmittance was recorded as a function of the sample position on the *Z*-axis (closed-aperture *Z*-scan). For measuring the NLO absorption, the *Z*-dependent sample transmittance was taken without the aperture (open-aperture *Z*-scan).

3. Results and discussion

3.1. Preparation

Complexes **1**, **3** and **4** were prepared in reasonable yield as shown in Scheme 1. They are soluble in most organic solvents and air stable in both solution and solid state. As shown in Scheme 2, complex **2** was prepared by I_2-oxidation of **1**, which was insoluble in most organic solvents but with marginal solubility in benzene.

3.2. Cyclic voltammetry

The electrochemical properties of complexes **1**, **3** and **4** (1×10^{-5} M) were investigated by cyclic voltammetry (Figs. S1–S3, Supporting information). For complex **1**, three redox couples are observed at $E_c = 0.009$, -0.447, and -1.06 V vs. s.c.e. The first process assigned to $[Ni(L)_2]^0/[Ni(L)_2]^-$ is quasi-reversible and is comparable to other nickel-dithiolene complexes [22–24]. The second process for $[Ni(L)_2]^-/[Ni(L)_2]^{2-}$ is irreversible. The third irreversible peak may be from the reduction of the dithiolene ligand. For complexes **3** and **4**, two irreversible redox couples are observed at $E_c = 0.489$ and -0.879 V, and 0.441 and -1.023 V vs. s.c.e., respectively. The first process corresponds to the $[Au(L)_2]^0/[Au(L)_2]^-$, and the second process may be assigned to the reduction of the dithiolene ligand.

3.3. ESR and NIR spectra

The solid ESR spectrum of complex **1** at 110 K is shown in Fig. 1a. The broadening of the two ESR signals at $g_1 = 2.062$ and $g_2 = 2.012$ is due to intermolecular interaction in the solid state [25]. The frozen glass ESR spectrum (Fig. 1b) of complex **1** in DMF at 110 K shows three peaks with $g_1 = 2.109$, $g_2 = 2.045$ and $g_3 = 2.004$. The

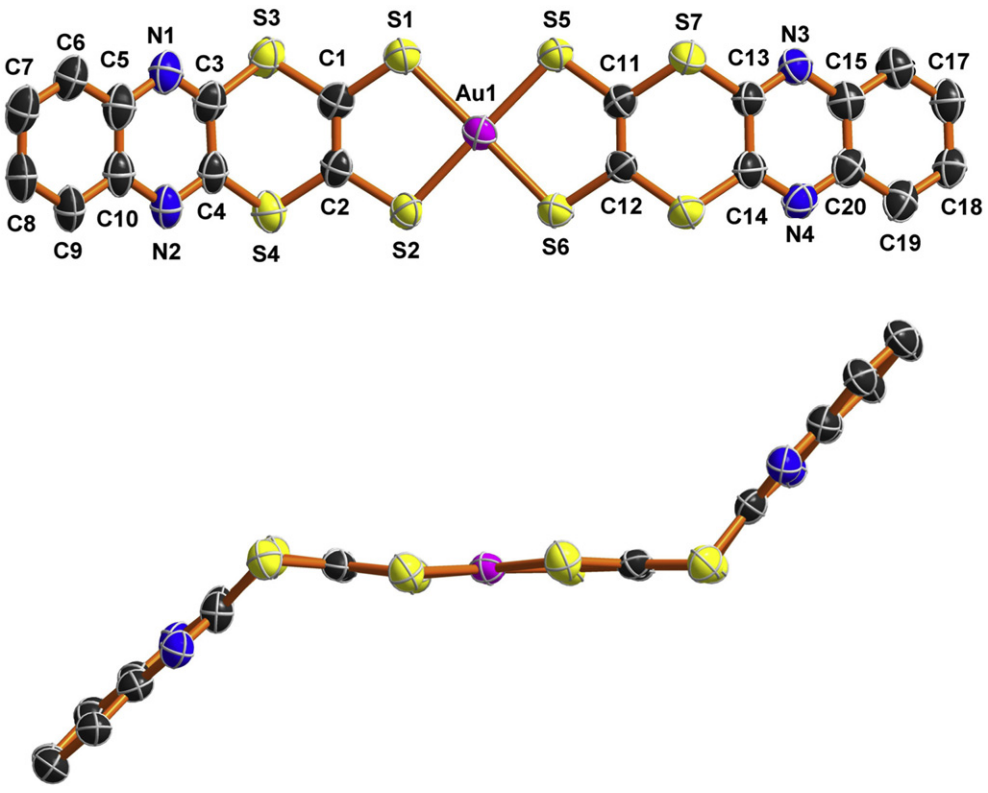

Fig. 5. Top and side views of $[Au(L)_2]^-$ with thermal ellipsoids at 30% probability level. Hydrogen atoms are omitted for clarity.

Table 2
Crystallographic data for compounds **1** and **3**.

	1	**3**
Empirical formula	$C_{36}H_{44}NiN_5S_8$	$C_{36}H_{44}AuN_5S_8$
M_r	862.01	1000.29
Cryst syst	Triclinic	Monoclinic
Space group	$P\bar{1}$	$P2_1/c$
a (Å)	11.2797(16)	8.4732(10)
b (Å)	14.916(2)	17.355(2)
c (Å)	24.424(4)	29.471(3)
α (°)	91.607(3)	90.00
β (°)	90.356(3)	105.564(4)
γ (°)	93.382(3)	90.00
V (Å^3)	4100.4(10)	4174.9(8)
Z	4	4
ρ_c (g cm^{-3})	1.396	1.592
$F(000)$	1804.0	2008.0
T/K	291(2)	291(2)
μ(Mo Kα)/mm^{-1}	0.914	3.957
Index ranges	$-11 \le h \le 13$	$-10 \le h \le 8$
	$-17 \le k \le 14$	$-20 \le k \le 20$
	$-29 \le l \le 28$	$-35 \le l \le 30$
GOF (F^2)	0.813	0.805
R_1,[a] wR_2[b] ($I > 2\sigma(I)$)	0.0786, 0.1464	0.0644, 0.1102

[a] $R_1 = \sum||C| - |F_c||/\sum|F_o|$.
[b] $wR_2 = [\sum w(F_o^2 - F_c^2)^2/\sum w(F_o^2)]^{1/2}$.

spectrum is similar to those of $[Ni(dmit)_2]^-$ [26] and $[Ni(medt)_2]^-$ [27], showing a rhombic g tensor.

The NIR spectra of complexes **1** and **2** are shown in Fig. 2, the characteristic long-wavelength transition for nickel complex is found at 1082 nm ($\varepsilon = 15\,000$ dm^3 mol^{-1} cm^{-1}), which is assigned to the $\pi-\pi^*$ transition [8]. The intense band at 316 nm ($\varepsilon = 50\,200$ dm^3 mol^{-1} cm^{-1}) is due to the $\pi-\pi^*$ transition of the ligand [28–30], and the band at 437 nm ($\varepsilon = 10\,000$ dm^3 mol^{-1} cm^{-1}) is reasonably ascribed to a Ni ← S charge transfer (c.t.) transition similar to other nickel(III) dithiolate complexes [31,32]. Complex **2** in benzene solution exhibits the absorption at 939 nm ($\varepsilon = 53\,500$ dm^3 mol^{-1} cm^{-1}). Table 1 lists the near-IR absorption maxima and absorbance of some typical nickel bis(dithiolene) complexes. Complex **3** exhibits a $\pi-\pi^*$ band at 311 nm ($\varepsilon = 40\,718$ dm^3 mol^{-1} cm^{-1}), and c.t. bands at 348 ($\varepsilon = 19\,141$ dm^3 mol^{-1} cm^{-1}) and 466 nm ($\varepsilon = 3490$ dm^3 mol^{-1} cm^{-1}). The near-IR band is absent in the corresponding gold complexes **3** and **4**, because the HOMO for these complexes are completely filled. The nickel and gold monoanionic complexes are not electronically similar systems.

In comparison with complex $[Ni(Pr^i_2timdt)_2]$ (Pr^i_2-timdt = 1,3-diisopropylimidazoline-2,4,5-trithione) [33–35] (Scheme 3) showing high absorption intensity at 1002 cm^{-1} ($\varepsilon = 80\,000$ dm^3 mol^{-1} cm^{-1}), the absorption band for complex **1** is much close to

Table 3
Selected bond lengths [Å] and angles [°] for compound **1**.

Ni1–S1	2.141(3)	Ni1–S2	2.144(3)	Ni1–S6	2.132(3)
Ni1–S5	2.133(3)	S1–C1	1.673(10)	S2–C2	1.699(10)
S5–C11	1.730(11)	S6–C12	1.684(10)	C1–C2	1.402(11)
S3–C1	1.762(10)	S4–C2	1.752(10)	C3–C4	1.400(13)
S3–C3	1.763(11)	S4–C4	1.753(11)	C11–C12	1.377(11)
S7–C11	1.752(11)	S8–C12	1.760(10)	S7–C13	1.753(12)
S8–C14	1.732(11)	C13–C14	1.441(13)		
S6–Ni1–S1	179.61(13)	S6–Ni1–S5	92.14(13)	S5–Ni1–S1	87.78(13)
S1–Ni1–S2	91.78(13)	S6–Ni1–S2	88.30(13)	C1–S1–Ni1	104.6(4)
C2–S2–Ni1	103.9(4)	C11–S5–Ni1	103.6(4)	C12–S6–Ni1	104.4(4)
C2–C1–S3	123.3(9)	C2–C1–S1	120.0(8)	C1–S3–C3	105.1(6)
S1–C1–S3	116.6(6)	C1–C2–S2	119.5(8)	C1–C2–S4	125.6(8)
S2–C2–S4	114.8(6)	C4–C3–S3	124.1(12)	C3–C4–S4	124.8(12)
C12–C11–S5	119.0(9)	C12–C11–S7	127.1(9)	S5–C11–S7	113.8(6)
C11–C12–S6	120.5(9)	C11–C12–S8	122.2(9)	S6–C12–S8	117.3(6)
C11–S7–C13	103.8(6)	C14–C13–S7	124.2(11)	C13–C14–S8	123.2(11)

Table 4
Selected bond lengths [Å] and angles [°] for compound **3**.

Au1–S1	2.282(3)	Au1–S2	2.300(3)	Au1–S5	2.305(3)
Au1–S6	2.282(3)	S1–C1	1.738(12)	S2–C2	1.739(12)
S5–C11	1.741(12)	S6–C12	1.754(12)	C1–C2	1.395(14)
S3–C1	1.747(12)	S4–C2	1.732(12)	S3–C3	1.756(15)
S4–C4	1.734(14)	C3–C4	1.469(17)	C11–C12	1.367(13)
S7–C11	1.755(11)	S8–C12	1.727(12)	S7–C13	1.754(13)
S8–C14	1.744(13)	C13–C14	1.476(16)		
S6–Au1–S1	178.74(12)	S6–Au1–S2	88.67(11)	S1–Au1–S2	90.47(12)
S6–Au1–S5	90.60(11)	S1–Au1–S5	90.29(12)	S2–Au1–S5	178.55(12)
C1–S1–Au1	102.0(5)	C2–S2–Au1	102.7(5)	C11–S5–Au1	100.9(4)
C12–S6–Au1	101.9(4)	C2–C1–S1	123.7(10)	C1–C2–S2	120.9(10)
S4–C2–S2	116.2(8)	C4–C3–S3	118.4(14)	C3–C4–S4	122.2(14)
C12–C11–S5	123.8(9)	C12–C11–S7	122.1(10)	S5–C11–S7	114.1(7)
C11–C12–S8	123.0(10)	C11–C12–S6	121.8(10)	S8–C12–S6	115.2(7)
C14–C13–S7	119.8(12)	C13–C14–S8	120.6(12)	C2–S4–C4	99.1(7)
C1–S3–C3	100.6(7)	C13–S7–C11	100.1(6)	C12–S8–C14	101.5(6)

1064 nm and 1079 nm at which Q-switching Nd–YAG and Nd–YAP lasers operate, respectively. Actually, the absorption intensity for **1** at 1064 nm and 1079 nm is 14 800 and 15 000 dm^3 mol^{-1} cm^{-1}. More importantly, it also exhibits good solubility in most organic solvents and high thermal and photochemical stabilities. Complex **1** is an excellent candidate as a near-IR dye for Q-switching neodymium lasers.

3.4. X-ray crystal structures

Single crystals suitable for X-ray structure analysis of compounds **1** and **3** were obtained from the recrystallization in acetone. Side and top views of $[Ni(L)_2]^-$ and $[Au(L)_2]^-$ are shown in Figs. 3 and 5, respectively. Final crystallographic data is listed in Table 2 and selected bond distances and angles for **1** and **3** are listed in Tables 3 and 4, respectively.

In complex **1**, the asymmetric unit consists of two crystallographically non-equivalent $[Ni(L)_2]^-$ anions and two $[n\text{-}Bu_4N]^+$ cations. The dihedral angle between the plane A (S1, S2, S5 and S6) and the plane B (S5, S6, S7 and S8) is about 6°, which is close to that in $[Ni(fcvdt)_2]^-$ [36]. The terminal 1,4-dithiin rings are folded up and down with the dihedral angle between the planes B and C (formed by C13, C14, N3 and N4) being about 26°. The two terminal phenyl rings are folded in opposite directions with an inversion center at the Ni position and show the chair-like conformation. As shown in Fig. 4, the anions form zig-zag chains along the b axis and a layered structure is further observed in the bc plane.

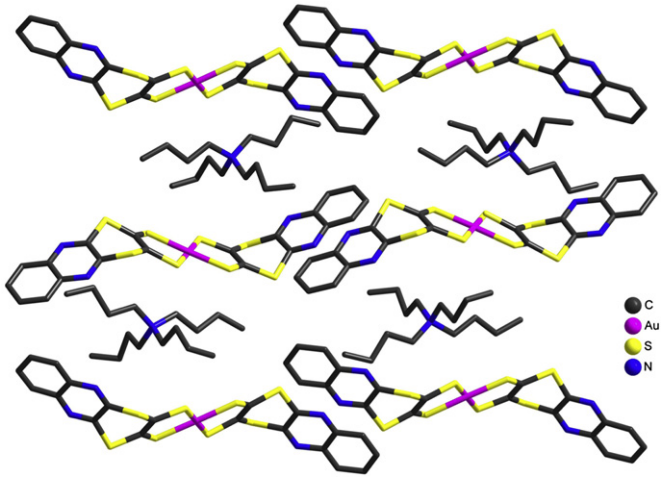

Fig. 6. The packing diagram of the anions in the unit cell of complex **3** looking along the a axis.

Table 5
Third-order non-linear optical date for some gold dithiolene complexes.

Complex	α_2 (m w^{-1})	n_2 (esu)	$\chi^{(3)}$ (esu)	Ref.
[*n*-Bu$_4$N][Au(L)$_2$]	2.22×10^{-10}	-4.83×10^{-11}	7.3×10^{-13}	This work
[Et$_4$N][Au(L)$_2$]	1.67×10^{-10}	-5.66×10^{-11}	7.4×10^{-13}	This work
[(C$_{12}$H$_{25}$)$_2$(Me)$_2$N] [Au(dmit) $_2$]			1×10^{-13}	12
[Me$_4$N][Au(dmit)$_2$]	2.5×10^{-11}	-2.8×10^{-12}	6.8×10^{-13}	6
[*n*-Bu$_4$N] [Au(dmit)$_2$]	1.82×10^{-11}	-5.00×10^{-12}	8.06×10^{-13}	7

In complex **3**, the asymmetric unit consists of one $[Au(L)_2]^-$ entity and one $[n\text{-}Bu_4N]^+$ cation. The dihedral angle between plane D (formed by S1, S2, S5 and S6) and plane E (formed by S1, S2, S3 and S4) is about 4°. The terminal 1,4-dithiin rings are folded up and down with the dihedral angle between planes E and F (formed by atoms C3, C4, N2 and N1) being about 48°, much larger than that in complex **1**. Fig. 6 shows the molecular packing diagram of complex **3**. The anions stack along the *a* axis while the cations occupy the holes between them.

The anions of complexes **1** and **3** are located separately from each other with no shorter intermolecular contact between the chalcogen atoms.

3.5. Non-linear optical properties

The third-order non-linear optical properties of the three complexes, at 532 nm, were measured by the *Z*-scan techniques as described earlier [37]. The results for some gold dithiolene complexes are summarized in Table 5. The *Z*-scan results for complexes **1**, **3** and **4** are shown in Figs. 7–9, respectively, where the filled circles related to the *Z*-scan data measured without the aperture and the open circles were the results obtained from dividing the *Z*-scan measured with the aperture by the *Z*-scan measured without the aperture. Since light transmittance (T) is a function of the sample's Z position (with respect to the focal point at $Z = 0$), Equations (1) and (2) [38–40] describe the typical and pure absorptive behavior of a hypothetical third-order NLO process, where α_0 is the linear absorptive coefficients index, τ is the time and L is the optical path length. The effective non-linear absorptive index α_2 of complexes **3** and **4** were calculated to be 2.2227×10^{-10} m w^{-1} and 1.6732×10^{-10} m w^{-1}, respectively, while the non-linear absorption of complex **1** is negligible.

$$T(Z) = \frac{1}{\sqrt{\pi} q(z)} \int_{-\infty}^{+\infty} \ln[1 + q(Z)] e^{-\tau^2} \, d\tau \quad (1)$$

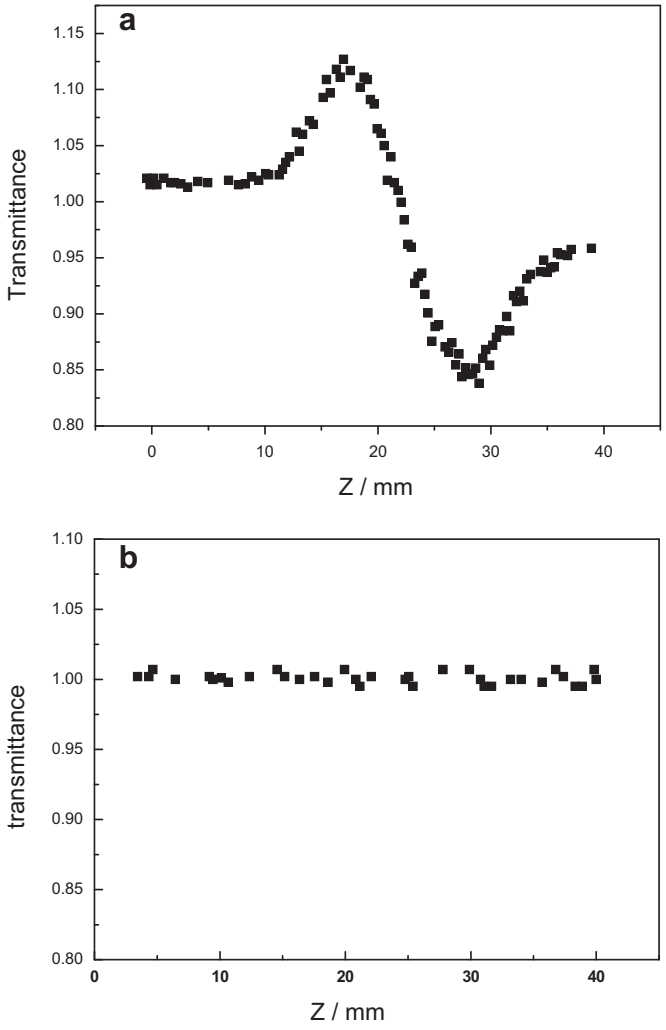

Fig. 7. The *Z*-scan result for complex **1** (2×10^{-4} M) showing the non-linear refraction (a) and the non-linear absorption (b).

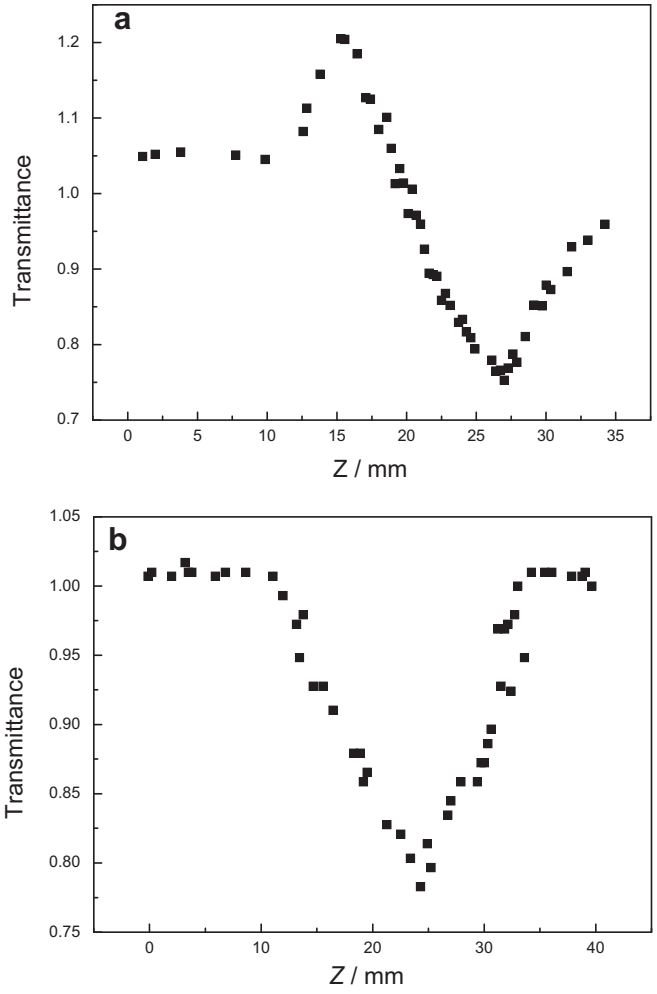

Fig. 8. The *Z*-scan result for complex **3** (2×10^{-4} M) showing the non-linear refraction (a) and the non-linear absorption (b).

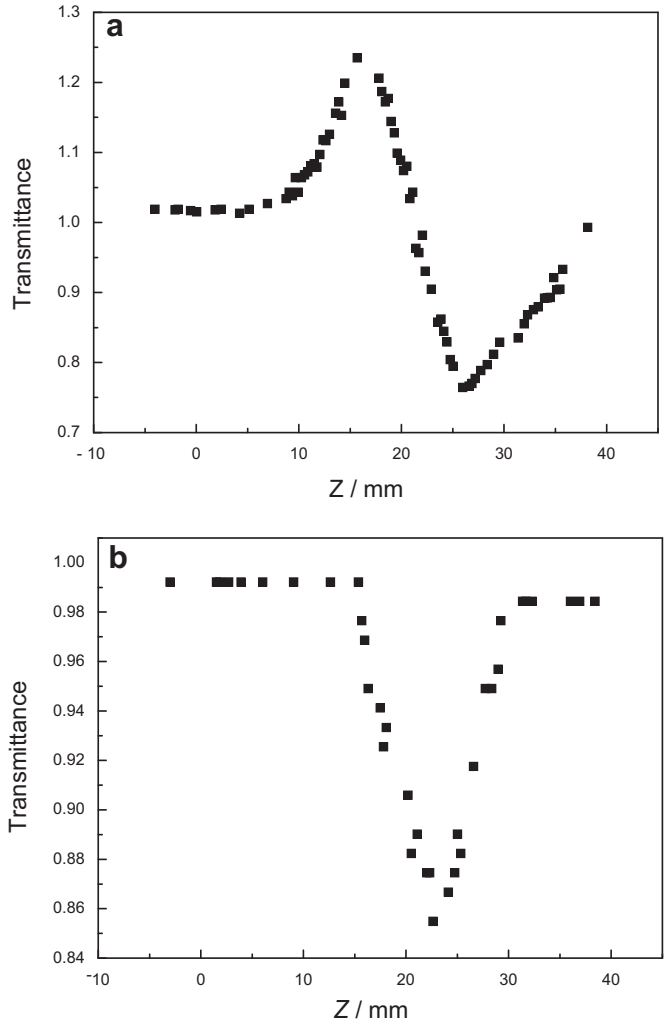

Fig. 9. The *Z*-scan result for complex **4** (2×10^{-4} M) showing the non-linear refraction (a) and the non-linear absorption (b).

$$q(Z) = \alpha_2 \frac{I_0}{1 + (Z/Z_0)^2} \frac{1 - e^{-\alpha_0 L}}{\alpha_0} \quad (2)$$

The non-linear refractive properties of these complexes were assessed under the closed-aperture configuration while the absorptive properties were assessed under the open-aperture configuration. The valley–peak pattern of the normalized transmittance curve under the closed-aperture configuration shows characteristic self-defocusing behavior of the samples **1**, **3** and **4**. The effective third-order non-linear refractive index n_2 of **1**, **3** and **4** can be derived from the difference between the normalized transmittance values at the valley and peak positions (ΔT_{V-P}) by using Equation (3) [37], where I is the peak irradiation intensity at focus and λ is the wavelength of the laser.

$$n_2 = \frac{\lambda \alpha_0}{0.812 \pi I (1 - e^{-\alpha_0 L})} \Delta T_{V-P} \quad (3)$$

From the different values between normalized transmittance at valley and peak portions, the NLO refractive index (n_2) were calculated to be -1.0357×10^{-17} m^2 W^{-1} (-3.37×10^{-11} esu) for complex **1**, -1.4377×10^{-17} m^2 W^{-1} (-4.83×10^{-11} esu) for complex **3**, and -1.6850×10^{-17} m^2 W^{-1} (-5.66×10^{-11} esu) for complex **4**. The negative values of the third-order non-linear refraction of the complexes also indicate that there are self-defocusing effects in the NLO refractive behaviors of these metal 1,2-dithiolene complexes.

According to the literature method [7], the third-order non-linear susceptibility $\chi^{(3)}$ of complexes **3** and **4** was estimated as 7.3×10^{-13} and 7.4×10^{-13} esu, respectively.

4. Conclusions

Two new nickel and two new gold bis(dithiolene) complexes have been synthesized and characterized. The third-order non-linear properties have been studied by using the *Z*-scan method. The nickel complex **1** is of special interest since it shows remarkable absorption in the near-IR region ($\lambda = 1082$ nm, $\varepsilon = 15\,000$ dm^3 mol^{-1} cm^{-1}), which is very close to 1064 nm (Nd–YAG lasers) and 1079 nm (Nd–YAP lasers). More importantly, it is well soluble in most organic solvents and exhibits high thermal and photochemical stabilities. Complex **1** can be an excellent candidate as a near-IR dye for Q-switching neodymium lasers and optical limiting (OL) materials.

Acknowledgments

This work was supported by the Major State Basic Research Development Program (Grants 2007CB925103 and 2011CB808704), the National Science Fund for Distinguished Young Scholars of China (Grant 20725104), the National Natural Science Foundation of China (Grant 21021062), and the Academician Work Station of Changzhou Trina Solar Energy Co., Ltd.

Appendix. Supplementary data

Supplementary data associated with this article can be found, in the online version, at doi:10.1016/j.dyepig.2011.08.003.

References

[1] Bousseau M, Valade L, Legros JP, Cassoux P, Garbauskas M, Interrante LV. Highly conducting charge-transfer compounds of tetrathiafulvalene and transition metal-"dmit" complexes. J Am Chem Soc 1986;100:1908–16.
[2] Garreau B, Chane K, Alary F, Bui T, Valade L. Neutral d^8 metal bis-dithiolene complexes: synthesis, electronic properties and applications. Coord Chem Rev 2010;254:1457–67.
[3] Arslanoğlu Y, Hamuryudan E. Synthesis and derivatization of near-IR absorbing titanylphthalocyanines with dimethylaminoethylsulfanyl substituents. Dyes Pigm 2007;75:150–5.
[4] Deplano P, Mercuri ML, Pilia L, Serpe A. Structure and properties of d^8-metal dithiolene complexes. John Wiley& Sons, Ltd; 2009. p. 879–928.
[5] Coe BJ. Nonlinear optical properties of metal complexes. Compr Coord Chem II 2004;9:621–87.
[6] Sun XB, Ren Q, Wang XQ, Zhang GH, Yang HL, Feng L, et al. Nonlinear optical properties of $[(CH_3)_4N]Au(dmit)_2$ using Z-scan technique. Chin Phys 2006;15:2618–22.
[7] Yang HL, Ji W, Ren Q, Wang XQ, Zhang FJ, He JJ. Study on third-order nonlinear optical properties of $[(C_4H_9)_4N]Au(dmit)_2$ using Z-scan technique. Proc SPIE 2009;7631. 76310V/1–76310V/7.
[8] Mueller-Westerhoff UT, Vance B, Yoon DI. The synthesis of dithiolene dyes with strong near-IR absorption. Tetrahedron 1991;47:909–32.
[9] Zuo JL, Yao TM, You F, You XZ, Fun HK, Yip BC. Syntheses, characterization and non-linear optical properties of nickel complexes of multi-sulfur 1,2-dithioiene with strong near-IR absorption. J Mater Chem 1996;6:1633–7.
[10] Bai JF, Zuo JL, Tan L, Ji W, Shen Z, Fun HK, et al. Synthesis, structure and optical limiting effect of two new nickel complexes containing strongly bound geometrically fixed multi-sulfur 1,2-dithiolene ligands showing remarkable near-IR absorption. J Mater Chem 1999;9:2419–23.
[11] Winter CS, Oliver SN, Manning RJ, Rush JD, Hill CAS, Underhill AE. Non-linear optical studies of nickel dithiolene complexes. J Mater Chem 1992;2:443–7.
[12] Wang SF, Huang WT, Zhang TQ, Yang H, Gong QH, Okuma Y, et al. Third-order nonlinear optical properties of didodecyldimethylammonium–Au(dmit)$_2$. Appl Phys Lett 1999;75:1845–7.
[13] Ray K, Weyhermuller T, Neese F, Wieghardt K. Electronic structure of square planar bis(benzene-1,2-dithiolato)metal complexes $[M(L)_2]^z$ (z = 2–, 1–, 0; M = Ni, Pd, Pt, Cu, Au): an experimental, density functional, and correlated ab initio study. Inorg Chem 2005;44:5345–60.
[14] Drexhage KH, Muller-Westerhoff UT. New Q-switch compounds for infrared lasers. IEEE J Quantum Electron 1972;8:759.

[15] Drexhage KH, Muller-Westerhoff UT. US Pat., 3743 964; 1973.
[16] Aragoni MC, Arca M, Cassano T, Denotti C, Devillanova FA, Frau R, et al. NIR dyes based on [M(R, R′timdt)$_2$] metal-dithiolenes: additivity of M, R, and R′ contributions to tune the NIR absorption (M = Ni, Pd, Pt; R, R′timdt = monoreduced form of disubstituted imidazolidine-2,4,5-trithione). Eur J Inorg Chem; 2003:1939–47.
[17] Steimecke G, Sieler HJ, Kirmse R, Hoyer E. 1.3-Dithiol-2-Thion-4.5-Dithiolat Aus Schwefelkohlenstoff Und Alkalimetall. Phosphorus Sulfur 1979;7:49–55.
[18] Varma KS, Edge S, Underhill AE. New symmetrical and unsymmetrical tetrathiafulvalene π-donors containing the dithiinoquinoxaline ring system. J Chem Soc Perkin Trans 1; 1990:2563–5.
[19] SAINT-Plus. Version 6.02. Madison, WI: Bruker Analytical X-Ray System; 1999.
[20] Sheldrick GM. SADABS. An empirical absorption correction program. Madison, WI: Bruker Analytical X-Ray Systems; 1996.
[21] Sheldrick GM. SHELXTL-97. Göttingen, Germany: Universität of Göttingen; 1997.
[22] Faulmann C, Errami A, Donnadieu B, Malfunt I, Legros JP, Cassoux P, et al. Metal complexes of dithiolate ligands: 5,6-dihydro-1,4-dithiin-2,3-dithiolato (dddt^{2-}), 5,7-dihydro-1,4,6-trithiin-2,3-dithiolato (dtdt^{2-}), and 2-thioxo-1,3-dithiole-4,5-dithiolato (dmit^{2-}). Synthesis, electrochemical studies, crystal and electronic structures, and conducting properties. Inorg Chem 1996;35:3856–73.
[23] Madhu V, Das SK. New series of asymmetrically substituted bis(1,2-dithiolato)-nickel(III) complexes exhibiting near IR absorption and structural diversity. Inorg Chem 2008;47:5055–70.
[24] Harrison DJ, Crisci AGD, Lough AJ, Kerr MJ, Fekl U. Nickel dithiolene chelate rings in a new role as η^5-coordinating ligands: synthesis, structural characterization, and redox reactivity of an "Fe_2Ni" bis-double-decker. Inorg Chem 2008;47:10199–201.
[25] You XZ. Structure and properties of coordination compounds. Beijing: Science Press; 1992. p. 315.
[26] Kirmse R, Stach J, Dietzsch W, Steimecke G, Hoyer E. Single-crystal EPR studies on nickel(III), palladium(III), and platinum(III) dithiolene chelates containing the ligands isotrithionedithiolate, o-xylenedithiolate, and maleonitriledithiolate. Inorg Chem 1980;19:2679–85.
[27] Yao TM, Zuo JL, You XZ. Syntheses and properties of the nickel complexes of 1,2-dithiolates medt and phdt. The crystal structure of [Bu_4N][Ni(medt)$_2$]. Polyhedron 1995;11:1487–94.
[28] Andersen OP, Perkins CM, Brito KK. Synthesis, structures, and electrochemistry of copper(II)–mercaptide complexes. Inorg Chem 1983;22:1267–73.
[29] Aoi N, Matsubayashi G, Tanaka T. Syntheses, spectroscopic, and electrochemical properties of dinuclear copper(II) complexes bridged by a single thiolate sulphur atom; X-ray crystal structures of [$Cu_2(L^1)_2(SC_6H_4Cl\text{-}4)$][$PF_6$] and [$Cu_2(L^2)_2(SC_6H_4CH_3\text{-}4)$][$ClO_4$]. J Chem Soc Dalton Trans; 1987:241–7.
[30] Hughey IV JL, Fawcett TG, Rudish SM, Lalancette RA, Potenza JA, Schugar HJ. Preparation and characterization of [rac-5,7,7,12,14,14,-hexamethyl-1,4,8,11-tetraazocyclotetradecane]copper(II) o-mercaptobenzoate hydrate, [Cu(tet b)(o-$SC_6H_4CO_2$)]·H_2O, a complex with a CuN_4S (mercaptide) chromophore. J Am Chem Soc 1979;101:2617–23.
[31] Matsubayashi G, Tanaka S, Yokozawa A. Crystal structures of [NBu^n_4]$_2$[M(C_3S_5)(C_3Se_5)](M = Ni or Pd) and properties of the nickel(II) complex. J Chem Soc Dalton Trans; 1992:1827–30.
[32] Dietzsch W, Rauer S, Olk RM, Kirmse R, Köhler K, Golič L, et al. Ligand exchange reactions between metal(II) chelates of different sulfur and selenium containing ligands IX. Exchange behavior of chelates of 1,3-dithiole-2-thione-4,5-dithiolate (dmit) and 1,1-dichalcogenolates. X-ray structure of Bu_4N[Zn(dmit)(Et_2dtc)]. Inorg Chim Acta 1990;169:55–62.
[33] Bigoli F, Deplano P, Devillanova FA, Lippolis U, Lukes PJ, Mercuri ML, et al. New neutral nickel dithiolene complexes derived from 1,3-dialkylimidazolidine-2,4,5-trithione, showing remarkable near-IR absorption. J Chem Soc Chem Commun; 1995:371–2.
[34] Bigoli F, Deplano P, Devillanova FA, Frraro JR, Lippolis V, Lukes PJ, et al. Syntheses, X-ray crystal structures, and spectroscopic properties of new nickel dithiolenes and related compounds. Inorg Chem 1997;36:1218–26.
[35] Arca M, Demartin F, Devillanova FA, Garau A, Isaia F, Lelj F, et al. Synthesis, X-ray crystal structure and spectroscopic characterization of the new dithiolene [Pd(Et_2timdt)$_2$] and of its adduct with molecular diiodine [Pd(Et_2timdt)$_2$]·I_2·$CHCl_3$ (Et_2timdt = monoanion of 1,3-diethylimidazolidine-2,4,5-trithione). J Chem Soc Dalton Trans; 1998:3731–6.
[36] Lee H-J, Noh D-Y. Syntheses, X-ray crystal structures and properties of di- and tetra-ferrocenyl nickel-bis(1,4-dithiin-5,6-dithiolate) complexes. J Mater Chem 2000;10:2167–72.
[37] Sheik-bahae M, Said AA, Van Stryland EW. High-sensitivity, single-beam n_2 measurements. Opt Lett 1989;14:955–7.
[38] Sherk-Bahae M, Said AA, Wei TH, Hagan DJ, Van Stryland EW. Sensitive measurement of optical nonlinearities using a single beam. IEEE J Quantum Electron 1990;26:760–9.
[39] Bondi A. van der Waals volumes and radii. J Phys Chem 1964;68:441–51.
[40] Said AA, Sheik-Bahae M, Hagan DJ, Wei TH, Wang J, Young J, et al. Determination of bound-electronic and free-carrier nonlinearities in ZnSe, GaAs, CdTe, and ZnTe. J Opt Soc Am B 1992;9:405–14.